Article

# Enhanced Hydrogen Storage on Li-Dispersed Carbon Nanotubes

W. Liu, Y. H. Zhao, Y. Li, Q. Jiang, and E. J. Lavernia

*J. Phys. Chem. C*, **2009**, 113 (5), 2028-2033 • Publication Date (Web): 12 January 2009

# Enhanced Hydrogen Storage on Li-Dispersed Carbon Nanotubes

**W. Liu,[†,‡] Y. H. Zhao,[†] Y. Li,[†] Q. Jiang,*[,‡] and E. J. Lavernia*[,†]**

*Department of Chemical Engineering and Materials Science, University of California, Davis, California 95616, and Key Laboratory of Automobile Materials, Ministry of Education, and Department of Materials Science and Engineering, Jilin University, Changchun 130022, China*

*Received: October 16, 2008; Revised Manuscript Received: December 2, 2008*

High storage capacity and a moderate binding strength are two important requirements that must be met for the successful development of hydrogen storage materials. In the present work we demonstrate that optimizing the number and position of dopants, a configuration of eight Li dispersed at the hollow sites above the hexagonal carbon rings, can lead to an extremely high $H_2$ storage capacity of 13.45 wt %. Moreover, our local density approximation calculations predict that the average adsorption energy is −0.17 eV/$H_2$, which is close to the lowest requirement (−0.20 eV/$H_2$) as proposed by the U.S. Department of Energy. The electronic analysis demonstrates two salient points, namely that the best dopants are those whose bands overlap strongly with those of $H_2$ and the nanotube simultaneously; second, all carbon atoms in the nanotube are fully ionized and thus the high capacity is attainable. These results provide insight into the binding mechanisms that govern hydrogen storage.

## 1. Introduction

Hydrogen ($H_2$) has been recognized as an attractive alternative energy carrier, which is lightweight, nonpolluting, highly efficient, and easily derived.[1,2] The so-called $H_2$ fuel economy, however, faces various hurdles, such as safe and reliable storage concepts that can be used to deliver and store $H_2$ in a cost-effective way.[3,4] Traditional storage approaches, such as compressed gas and liquefaction, are not suitable for $H_2$, because of safety issues and relatively high energy costs associated with these approaches.[5] More recently, efforts have been devoted toward the development of suitable hydrogen storage materials with high storage capacity and fast kinetics for on-board applications.[6−8] A review of the current literature shows that carbon-based nanostructures, including nanotubes,[9−13] fullerenes,[14−17] graphenes,[13,18−20] and nanoscrolls[21,22] have emerged as attractive candidate hydrogen storage materials. Noteworthy is the fact that far more hydrogen can be adsorbed in structures with curvature, such as those in carbon nanotubes, than on the flat surface of graphite at low temperatures, for example. This behavior is related to the curvature of the surface and the related higher number of carbon atoms interacting with the $H_2$ molecule.[1] Moreover, metal atoms are often decorated on the pure nanostructures to enhance their storage capacity in case of practical applications.[3,23,24]

Storage capacity and binding strength represent the two most basic parameters that can be used to characterize a $H_2$ storage material. In the case of the former parameter, the higher the better, whereas for the latter case, a moderate bonding strength between the physisorbed and the chemisorbed states[5,25] is ideal since ultimately both storage and release of $H_2$ will be necessary. In terms of the above two requirements, the U.S. Department of Energy (DOE) proposed goals, such that the $H_2$ capacity should exceed 6.0 wt %, and that the adsorption energy $E_{ad}$ should be between −0.20 and −0.70 eV/$H_2$ at room temperature.[26,27] Table 1 summarizes the storage capacity and average binding strength of the $H_2$ storage materials as published in the literature. Among them, the highest storage capacities experimentally obtained in Li- and K-doped carbon nanotubes were reported by Chen et al. as 20 and 14 wt %, respectively,[28] while other authors found that the storage increase was due to the presence of water impurities in the experiments[29,30] and the real uptake capacity of these was only about 2 wt %.[29] In the case of DFT simulations, Durgun et al.[8] predicted that a single ethylene ($C_2H_4$) molecule can form a stable complex with two transition metals such as Ti, which can adsorb ten $H_2$ molecules and lead to a high storage capacity of ∼14 wt %. However, only 6.1 wt % can be achieved if the $C_2H_4Ti_2$ complexes were incorporated in a graphene layer, in order to prevent forming a possible polymer phase during recycling. In addition, Sun et al.[25] showed that the highest $H_2$ capacity is about 13 wt % in a fullerene cage with 12 Li atoms capped onto the pentagonal faces, while its average $E_{ad}$ is −0.075 eV/$H_2$ from the generalized gradient approximation (GGA) with the Perdew−Wang 1991 functional.[31]

**TABLE 1: Storage Capacity in wt % and Average Binding Strength $E_{ad}$ in eV/$H_2$ of the $H_2$ Storage Materials Available in the Literature**

| materials | capacity | $-E_{ad}$ | method | reference |
|---|---|---|---|---|
| Li-doped carbon nanotube | ∼20 | | | |
| K-doped carbon nanotube | ∼14 | \ | exp. | Chen[28] |
| pure carbon nanotube | 4.2 | \ | exp. | Liu[11] |
| Li-doped graphene | 6.5 | \ | DFT | Deng[47] |
| Ti-doped carbon nanotube | 7.7 | 0.18 | DFT | Yildirim[24] |
| 12-Li-doped fullerene | 13 | 0.08 | DFT | Sun[25] |
| Ti−$C_2H_4$ complex | ∼14 | 0.29−0.49 | | |
| Ti−$C_2H_4$ on graphene | 6.1 | 0.41 | DFT | Durgun[8] |
| covalent-bonded graphene | 5 | 0.10 | DFT | Park[20] |
| Carbon nanoscroll | 3 | \ | DFT | Mpourmpakis [22] |
| $TiB_2$ nanotubes | 5.5 | 0.20 | DFT | Meng[3] |
| pure carbon nanotubes | 7 | \ | Exp. | Nikitin[7] |
| giant fullerene cage $C_{720}$ | 10 | \ | DFT | Pupysheva[14] |
| 8-Na-doped $C_{60}$ fullerene | 9.5 | 0.08 | DFT | Chandrakumar[16] |
| 32-Ca-doped $C_{60}$ fullerene | 8.4 | 0.2−0.4 | DFT | Yoo[17] |

* To whom correspondence should be addressed. (Q.J.) Tel: +86 431 85095371. Fax: +86 431 85095876. E-mail: jiangq@jlu.edu.cn. (E.J.L.) Tel: +1 530 752 0554. Fax: +1 530 752 8058. E-mail: lavernia@ucdavis.edu.
† University of California.
‡ Jilin University.

10.1021/jp8091418 CCC: $40.75 
Published on Web 01/12/2009

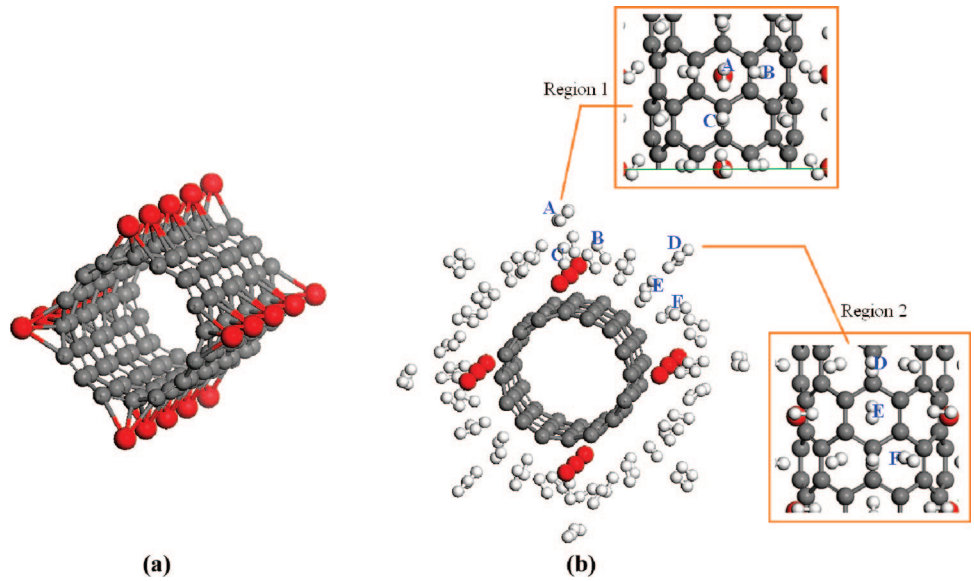


**Figure 1.** Schematic plots for the storage material: (a) the Li-dispersed carbon nanotube with Li:C = 1:8, and (b) the relaxed $(H_2)_{64}/Li_8/C_{64}$ system. The two insets show the fine views of regions 1 and 2, which indicate the areas close to and far from Li atoms, respectively. The red, gray, and white spheres represent Li, C, and H atoms, respectively.

On the basis of the above results, one may hypothesize that the uptake capacity will increase if more dopants are added. In addition, the binding would be strengthened if more charges are transferred between the dopants and nanostructures. Obviously, the latter can also be addressed by adding more dopants with concomitant additional charges available for electronic transfer. To examine the validity of this hypothesis, a multi-Li decorated carbon nanotube ($Li_8/C_{64}$, where the subscript indicates the number of the atom in a unit cell) is established as a model material in the present study. Although a number of studies in the literature show the effect of Li doping for different ratios,[12,16,25,32−35] our Li:C = 1:8 is quite moderate and moreover strictly obeys the doping rules for high coverage metals,[36,37] which makes it possible for us to achieve a relatively high storage capacity. This is because on one hand too few metal atoms cannot fully ionize the carbon atoms and thus cannot adsorb adequate $H_2$ molecules.[12,16,33,34] On the other hand, too many metal atoms (especially the heavy metals such as Ti) will considerably increase the self-weight of the storage material without apparent enhancement of ionizing carbon atoms.[3] In addition, metals intend to aggregate into clusters when their concentration is quite large, which may significantly reduce the hydrogen uptake.[38] Inspection of the published literature implies that most prior studies were centered on the problem of tight adsorption around a dopant[19,24] but ignored the remaining areas distant from the metal atoms. In this work, both regions are systematically studied, and our calculations demonstrate that each carbon atom can be fully ionized to store one $H_2$ molecule, which results in the maximum physisorption storage of $H_2$ where $H_2$ molecules are adsorbed as one layer. Moreover, specific attention is paid to the charge redistribution and orbital hybridization before and after Li doping. Our goal is to provide a new fundamental insight into the underlying mechanisms as well as the physical properties that are required for hydrogen storage. Since pure carbon nanotubes are not good candidate materials for hydrogen storage with $E_{ad} = -0.02$ to $-0.10$ eV/$H_2$, our work will examine the critical question of whether the storage ability of a carbon nanotube can be significantly enhanced.

In this contribution, 64 $H_2$ molecules are stored by an eight-Li-decorated single wall carbon nanotube. The adsorption structures are determined in terms of their corresponding $E_{ad}$ values. Two other systems are also calculated to render comparisons, where a single $H_2$ molecule is adsorbed on a pure, and on a one-Li-doped nanotube. In addition, the variations of geometry and energy are interpreted on the basis of the electronic analysis.

## 2. Computational Framework

The unrestricted spin-polarized density functional theory (DFT) calculations are carried out by the DMol$^3$ code, which uses numerical functions on an atom-centered grid as its atomic basis.[39,40] The all-electron (AE) core treatment and a double numeric basis with polarization (DNP) set are adopted. Although the local density approximation (LDA) generally overestimates the $H_2$ binding strength, prior works have proven that the physisorption results obtained from LDA are in substantial agreement with experiments.[18,41] The GGA, on the other hand, usually renders significantly smaller or even repulsive interactions.[42,43] In fact, LDA has been preferred as a reliable and computationally efficient functional to study the systems involving the van der Waals interactions.[42,44,45] Taking these in mind, LDA with the Perdew−Wang (PWC) method is utilized as the exchange-correlation functional throughout the paper.[31] The $k$-point is set to $1 \times 1 \times 5$, the smearing is 0.002 Ha (1 Ha = 27.2114 eV), and the global orbital cutoff radius is 4.4 Å for all calculations.

A storage model composed of Li-doped zigzag (8,0) carbon nanotube is built and depicted in Figure 1a. Noteworthy, the specific doping ratio of Li:C = 1:8 is not established a priori but arrived at "naturally" on the basis of the structure of the nanotube and the rule for decorating metals. In our simulation, the length of the tube equals twice the periodicity of the nanotube, and thus there are totally 64 carbon atoms in the unit cell.[46] Thereafter the Li metals are decorated above the hexagonal rings in the tube. In this case, although more Li atoms may lead to a larger storage capacity, our doping follows the rule that each carbon atom has a maximum of one dopant.[36,37] This hypothesis ensures that the Li−Li distance is sufficiently large without clustering of Li on the nanotube. Thus, at most eight Li atoms can be decorated into this 64 C unit cell where

Li:C = 1:8. Noteworthy, the entire structure deforms severely if all the neighboring six hexagon rings are occupied by Li while the metals delocalize from the center of the hollow sites and intend to aggregate into a cluster. This result agrees with a prior suggestion that the doping concentration of Li:C be less than 1:3 to shun the Li segregation on graphenes and nanotubes.[47] In fact, no Li aggregation was observed throughout the calculations reported here. As shown in Figure 1a, four lines of Li atoms are dispersed symmetrically at the hollow positions above the hexagonal rings. To check the stability of our models, the binding strength $E_b$ between the Li and the nanotube are determined. The calculated value of $E_b = -1.82$ eV/atom is lower than the heat of formation for the Li atom in the gas phase, which is $-1.62$ eV/atom.[48] Another possible doping site was also considered, and in this case, the Li atoms of a given row are placed not in a line but alternating between two adjacent lines. After full relaxation, it is found that the new doped system possesses a slightly lower energy ($E_b = -1.86$ eV/atom) than that corresponding to the geometry in Figure 1a ($E_b = -1.82$ eV/atom). Nevertheless, since this energetic difference is small (merely ~2%), the doping of our present model should also be energetically favorable. Sixty-four $H_2$ molecules are adsorbed around the above $Li_8/C_{64}$ model, where all initial molecules are parallel to the nanotube. To avoid the interactions from neighboring molecules, a cubic supercell of 30 × 30 × 8.52 Å$^3$ is used. For simplicity, this system is named as $(H_2)_{64}/Li_8/C_{64}$, which may render a gravimetric storage as high as 13.45 wt %. For a comparison purpose, the one-Li-doped ($H_2/Li/C_{64}$) and the no-Li-doped ($H_2/C_{64}$) storage systems are also simulated.

To explain the configurations of the relaxed molecules in Figure 1b, the interactions between a single $H_2$ molecule and the $Li_8/C_{64}$ models are investigated. Three possible adsorption sites exist around a dopant, which are the atop site ($H_2$ lies above a Li atom), the bridge site ($H_2$ located besides a Li atom), and the middle site ($H_2$ located between two neighboring Li atoms). Since each $H_2$ molecule can be vertical or parallel above the phenyl bond or phenyl center, there are totally six initial adsorption structures for the $H_2/Li_8/C_{64}$ system: atop parallel (AP), atop vertical (AV), bridge parallel (BP), bridge vertical (BV), middle parallel (MP), and middle vertical (MV). $H_2$ is docked into the vacuum with an initial bond length $d_{H-H} = 0.74$ Å.[49] The storage is physisorption with accompanying van der Waals forces, and thus $H_2$ keeps its molecular identity.[50] The adsorption energy $E_{ad}$ is defined as the negative of the value obtained by subtracting the total energy of the fragments from the adsorbed system at the equilibrium geometry, namely,

$$E_{ad} = (E_t - E_{mLi+C} - nE_{H_2})/n \quad (1)$$

where "$m$" and "$n$" indicate the numbers of Li atoms and $H_2$ molecules, respectively. The subscripts "t", "$m$Li+C" and "$H_2$" denote the total amount of the considered system, the corresponding storage material, and the free $H_2$ gas, respectively. Since one $n$ is located in the denominator, the corresponding $E_{ad}$ is an average value with the unit of eV/$H_2$. To check the convergence of our accuracy settings, taking the BV site as an example, the calculated $E_{ad}$ value is $-0.29$ eV/$H_2$ when the $k$-point, smearing, and cutoff radius are 1 × 1 × 3, 0.005 Ha, and 4.4 Å, respectively. The result decreases to $-0.30$ eV/$H_2$ when the settings are increased to 1 × 1 × 5, 0.002 Ha, and 4.4 Å. No change was found when settings are further increased to 1 × 1 × 6, 0.002 Ha, and 5.5 Å.

In addition, to clarify the electronic nature of Li-doping on the $H_2$ storage in carbon nanotubes, plots of density of states (DOS) and electron densities, as well as the Hirshfeld charge analysis, are determined and discussed. In our DOS plots, the Fermi energy $E_F$ is set to zero, which is defined as the energy where a half of the possible energy levels in the band are occupied by electrons in terms of the Fermi−Dirac statistics.[51]

## 3. Results and Discussion

The relaxed geometry for $(H_2)_{64}/Li_8/C_{64}$ system is shown in Figure 1b. A general observation is that the positions of $H_2$ change considerably, and the molecules are distributed randomly in comparison with those in the initial structure. Some regularity can also be observed in the configurations studied. Two insets made in this figure show detailed views, where region 1 (or 2) indicates the area that is close to (or far from) the Li atoms. More attention is paid to the former, where three $H_2$ named "A", "B", and "C" indicate the molecules located at the atop, bridge, and middle sites, respectively. It is discernible that the $H_{2A}$ molecules are still parallel to the dopants. The $H_{2B}$ molecules tilt spontaneously after relaxation and form a ~60° angle to the horizontal plane. A similar phenomenon can also be observed in $H_{2C}$, but renders a perpendicular angle to the C−C bond. This is understandable since the $H_{2C}$ located at the middle point of the two dopants would obtain symmetrical interactions. The distances between the molecules and Li have the sequence of A > B > C, which implies that $H_{2A}$ (or $H_{2B}$) should have the weakest (or strongest) binding in the three sites (this will be confirmed by the following $E_{ad}$ results for the $H_2/Li_8/C_{64}$ system). In region 2, the $H_{2D}$ molecule located above the C−C bond shows the longest distance from the nanotube. The $H_{2E}$ moves to the center of the hexagonal ring and lies parallel to the nanotube. In addition, the $H_{2F}$ molecules tilt and occupy all neighboring rings of $H_{2E}$. $E_{ad} = -0.17$ eV/$H_2$, which is close to the lowest binding requirement of $-0.20$ eV/$H_2$. From Figure 1b, one may assume that the outer $H_{2A}$ and $H_{2D}$ molecules escape from the storage materials, even though the uptake capacity of 10.51 wt % is much larger than that of 6.0 wt % from the DOE.

The calculated $E_{ad}$ values for the $H_2/Li_8/C_{64}$ systems are listed in Table 2. For the atop site, $E_{ad} = -0.15$ and $-0.02$ eV/$H_2$ for the AP and AV structures, respectively. Thus, the molecule prefers to be parallel because a lower energy state corresponds to a more stable configuration, which consists with the $H_{2A}$ configuration in Figure 1b. The bridge site corresponds to the $H_{2B}$ position, $E_{ad} = -0.30$ eV/$H_2$ and the relaxed $H_2$ changes from BP to BV spontaneously. Interestingly, this H−H bond is not absolutely vertical to the C−C bond, just like the conditions in Figure 1b. If the above value is selected as a reference, the binding strength at the middle site is 16.67% lower. Figures 2a to 2c shows the relaxed structures at the three sites, from which we can see that all of them correspond to the configurations of $H_2$ in Figure 1b.

The geometric parameters of the $H_2/Li_8/C_{64}$ system are also listed in Table 2. From this table, both the atomic distances $d$ of Li−H and Li−C are the shortest among the three sites. Thus, the binding strength between the $H_2$ and Li is inversely proportional to their corresponding $d$ values. In comparison with $d_{Li-C} = 1.48$ Å for the H-free $Li_8/C_{64}$ model, the entire system is noted to expand after hydrogen storage. For the free $H_2$ gas, our determined $d_{H-H} = 0.77$ Å is only 4.05% lower than those obtained from experiments.[49] All the H−H bonds elongate to 0.78−0.80 Å after adsorption due to the charge redistribution.[52] In addition, $Ø_x > Ø_y$ confirms the attractions between the $H_2$ molecules and the substrates, where $Ø_x$ and $Ø_y$ indicate the diameters of the nanotube along the horizontal and vertical directions, respectively.

**TABLE 2: Computed Adsorption Energy $E_{ad}$ Values in eV/$H_2$, and Geometric Parameters in Angstroms (atomic distance $d$, and diameters Ø of the nanotubes) for the $H_2/Li_8/C_{64}$ System[a]**

| structure | | $H_2/Li_8/C_{64}$ $-E_{ad}$ | $d_{Li-H}$ | $d_{Li-C}$ | $d_{H-H}$ | $Ø_x$[d] | $Ø_y$[d] | $H_2/Li/C_{64}$, $-E_{ad}$ | $H_2/C_{64}$, $-E_{ad}$ |
|---|---|---|---|---|---|---|---|---|---|
| bridge | BP | 0.30[b] | 1.91 | 1.49 | 0.79 | 6.36 | 6.35 | 0.22 | 0.06 |
| | BV | 0.30 | | | | | | 0.24 | 0.07 |
| atop | AP | 0.15 | 1.98 | 1.51 | 0.78 | 6.37 | 6.35 | 0.21 | 0.10 |
| | AV | 0.02 | | | | | | 0.21[e] | 0.09 |
| middle | MP | 0.25[c] | 1.98 | 1.51 | 0.80 | 6.38 | 6.33 | – | – |
| | MV | 0.25 | | | | | | – | – |

[a] The $E_{ad}$ values for the $H_2/C_{64}$ and $H_2/Li/C_{64}$ systems are also listed for a comparison purpose. [b] $H_2$ molecule converts spontaneously from BP to BV configuration after full relaxation. [c] $H_2$ molecule tilts at the MP site after full relaxation. [d] The subscripts "$x$" and "$y$" indicate the diameter values along the horizontal and vertical directions. [e] $H_2$ molecule changes spontaneously from AV to AP after full relaxation.

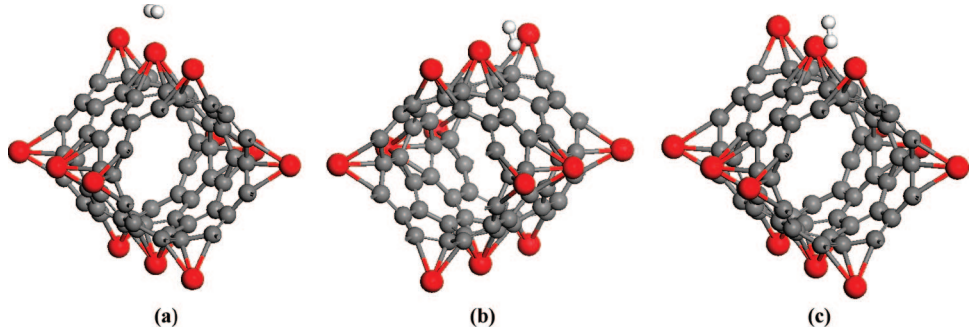


**Figure 2.** The relaxed configurations for a single $H_2$ molecule adsorption on the eight-Li-decorated nanotube at (a) atop site, (b) bridge site, and (c) middle site, respectively. The red, gray, and white spheres represent Li, C, and H atoms, respectively.

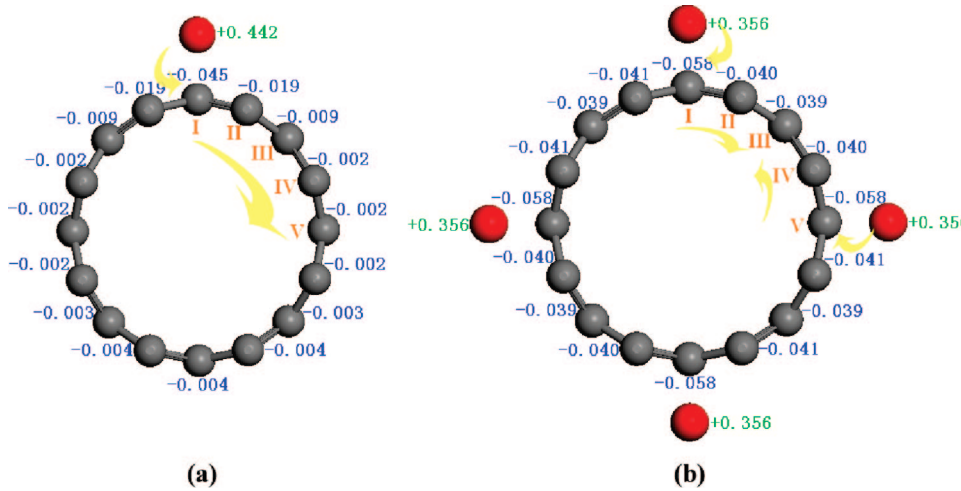


**Figure 3.** The Hirshfeld charge analysis for the atoms in the cross-section of storage materials: (a) the one-Li-doped carbon nanotube, and (b) the eight-Li-doped carbon nanotube, where the unit of the atom charge is one electron charge $e$. The red and gray spheres represent Li and C atoms, respectively. The yellow arrow lines indicate the possible charge flow directions within the systems.

Table 2 also gives calculated $E_{ad}$ values for the $H_2/C_{64}$ and $H_2/Li/C_{64}$ systems. It is discernible that the binding strength between a single $H_2$ and outer surface of a pure nanotube is very weak and that the physisorbed bond can easily be broken.[53] In addition, this system can be used to explain the geometry of the region 2 in Figure 1b. For example, AP is more stable than AV for the $H_2/C_{64}$ system, which agrees with the $H_{2E}$ configuration in Figure 1b. Comparing the values in Table 2, AP is the most preferred adsorption site in the $H_2/C_{64}$ system, while BV is the one in the $H_2/Li/C_{64}$ and $H_2/Li_8/C_{64}$ systems, whose corresponding $E_{ad}$ values are −0.10, −0.24, and −0.30 eV/$H_2$, respectively. Thus, the binding strength can be enhanced by introducing more dopants.

To understand the reasons why multiple Li decorated carbon nanotube can significantly enhance the uptake capacity of the carbon nanotubes, Hirshfeld charge analysis is carried out for the one-Li-doped and eight-Li-doped storage models. Figure 3a for the former shows that the Li dopant becomes a cation following decoration, whereas all C atoms in the cross-section carry negative charges. Among them, the $C_I$ obtains the largest amount of electrons from Li and carries −0.045 $e$. However, this value decreases gradually and rapidly when the charges "flow" away from the metal. As shown in this plot, the charges carried by the $C_{II}$, $C_{III}$, $C_{IV}$, and $C_V$ are only −0.019, −0.009, −0.002, and −0.002 $e$, respectively. Therefore, although the electron transfers from the metal to the nanotube, it is localized within small areas,[12] which brings out a small uptake capacity for the one-Li-doped model.

It is readily seen from Figure 1b that the $H_2$ molecules are adsorbed not only on the Li atoms, but also on the carbon nanotube. One may doubt this molecular distribution since the binding strength between $H_2$ and the pure carbon nanotube

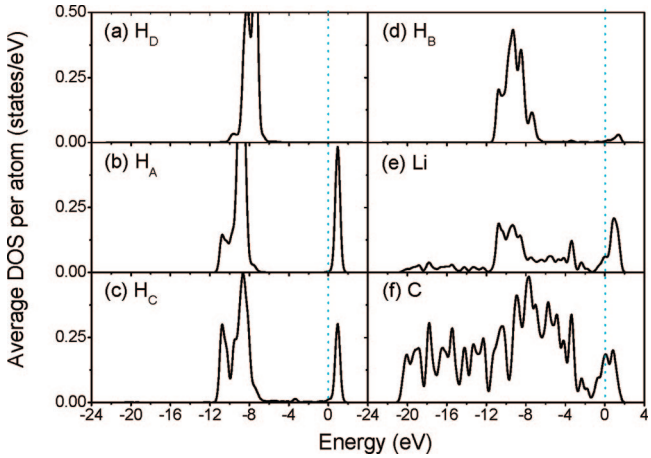


**Figure 4.** The average density of states (DOS) plots per atom for the $(H_2)_{64}/Li_8/C_{64}$ system in Figure 1b: (a) $H_D$, (b) $H_A$, (c) $H_C$, (d) $H_B$, (e) Li, and (f) C in the carbon nanotube. The subscripts have the same meanings as those in Figure 1b. The Fermi level $E_F$ is set to zero and indicated by a dotted line.

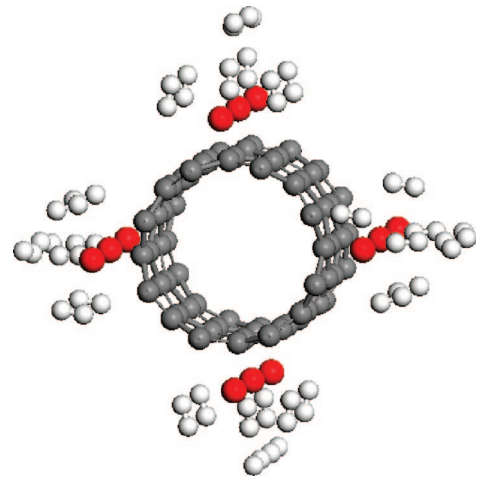

**Figure 5.** Schematic plots for the relaxed $(H_2)_{32}/Li_8/C_{64}$ system, where all 32 $H_2$ molecules are located around the Li dopants. The red, gray, and white spheres represent Li, C, and H atoms, respectively.

should be very weak. Here, the essential reason is that all carbon atoms participate in the electron transfer, and thus the carbon nanotube in our model differs from the pristine one. As shown in Figure 3b, differing from the one-Li-doped model, eight Li dopants simultaneously "pour" electrons into the carbon nanotube, and every C atom thus can get "enough" charges. The charge differences between the C atoms are not as significant as those in the $Li/C_{64}$ system, where $C_I$ (or $C_V$), $C_{II}$ (or $C_{IV}$), and $C_{III}$ carry $-0.058$, $-0.040$, and $-0.039$ $e$ charges, respectively. These render an extensive heteropolar bonding between the C atoms and the Li dopants, which results in production of extra dipole moments with a high $H_2$ uptake capacity.

To further understand the electronic hybridization behavior, the DOS plots are determined and shown in Figure 4 for the $(H_2)_{64}/Li_8/C_{64}$ system. Figure 4a shows the band of $H_D$, which has the weakest binding strength among the six $H_2$ sites and nearly releases from the storage media. If the $H_D$ is selected as a reference, the main peaks of $H_A$, $H_C$, and $H_B$ shift toward lower energies (move left) from $-7.42$ to $-8.66$, $-8.71$, and $-9.31$ eV in turn; see Figures 4a to 4d. This confirms again that the $H_2$ molecule has the binding sequence of bridge > middle > atop. Comparing Figures 4d with 4e, the peaks of Li located at $-10.75$, $-9.33$, $-8.52$, and $-7.47$ eV hybridize with the bridge H in the lower energy range, where the $\sigma$ bonding of the $H_2$ molecule overlaps with the Li-2s orbital at $-9.33$ eV. On the other hand, the bands of Li interact with those of C at the higher energy range, where a sharp peak can be observed around $-3.37$ eV, see Figures 4e and 4f. This suggests that Li acts as a "bridge" in this reaction, which interacts with the molecule and the carbon nanotube simultaneously. This result rationalizes the observation that Li dopants have a large influence in hydrogen storage systems. In fact, the Li atom will partially donate its valence electron to the carbon nanotubes, which binds $H_2$ in a molecular form due to the polarization mechanism.[25] This is confirmed by our Hirshfeld charge analysis that every Li carries a charge of $+0.356$ $e$ in the $Li_8/C_{64}$ system.

Although our $(H_2)_{64}/Li_8/C_{64}$ system can reach the highest capacity of 13.45 wt %, its $E_{ad}$ of $-0.17$ eV/$H_2$ is slightly higher than the lowest requirement proposed by the DOE. Obviously, a more ideal case is that both the storage capacity and the average $E_{ad}$ value can simultaneously achieve the goals, namely $E_{ad} < -0.20$ eV/$H_2$ with a capacity being larger than 6.0 wt %. This might be realized if the weak $H_2$ adsorption sites are excluded in our $Li_8/C_{64}$ system. To examine this hypothesis, all of the initial $H_2$ molecules were placed around the Li dopants, with the assumption that these areas have stronger $H_2$ storage ability than those between the two lines of the dopants. In this case, there are only 32 $H_2$ molecules located around the $Li_8/C_{64}$ model, where all initial molecules are also parallel to the nanotube. Thus, a half capacity of 6.72 wt % compared with the prior $(H_2)_{64}/Li_8/C_{64}$ model is realized, being still larger than the lowest requirement of 6.0 wt %. As shown in Figure 5, similar relaxed configurations can be found between the $(H_2)_{32}/Li_8/C_{64}$ and the $(H_2)_{64}/Li_8/C_{64}$ systems, namely that the $H_{2A}$ molecules are still parallel to the dopants, while the $H_{2B}$ and $H_{2C}$ molecules tilt spontaneously after relaxations. For this system, the simulated result shows that $E_{ad} = -0.20$ eV/$H_2$.

Noteworthy, the variation of the average $E_{ad}$ value is not very significant, although half of the capacity was sacrificed. This result can be interpreted by the charge analysis data. As shown in Figure 3b, the $C_{III}$ value is nearly the same as those of $C_{II}$ and $C_{IV}$, which implies that the areas between two lines of Li dopants are not as weak as we had expected. This is presumably because the charge transfer from the Li dopants to the nanotube will finally "converge" at the $C_{III}$ atom (as the arrow lines indicate in plot b). This is the reason why the $(H_2)_{64}/Li_8/C_{64}$ system should be a good candidate to achieve a high $H_2$ uptake capacity where there exist stronger binding zones everywhere.

## 4. Conclusions

In conclusion, DFT calculations indicated that we can obtain a high uptake $H_2$ capacity of 13.45 wt %, comparable with the DFT calculated highest value reported in literature, by optimizing the number and position of Li dopants on carbon nanotube, i.e. eight Li dispersed at the hollow sites above the hexagonal carbon rings. Geometric analysis shows that the $H_2$ molecules prefer to be parallel at the atop site, while vertical at the bridge and middle sites. The average $H_2$ bonding strength of the eight-Li-doped carbon nanotube is $-0.17$ eV/$H_2$, close to the lowest requirement ($-0.20$ eV/$H_2$) proposed by U.S. Department of Energy. In addition, the charge analysis results showed that no markedly weak binding zones exist in the $(H_2)_{64}/Li_8/C_{64}$ model, which supports this model being a good storage media for $H_2$.

**Acknowledgment.** W. Liu and Q. Jiang acknowledge financial support from the National Key Basic Research and Development Program of China (Grant No. 2004CB619301)

and the "985 Project" of Jilin University. Y. H. Zhao, Y. Li, and E. Lavernia would like to acknowledge support by the Office of Naval Research of the USA (Grant No. N00014-08-1-0405) with Dr. Lawrence Kabacoff as program officer.

## References and Notes

(1) Schlapbach, L.; Züttel, A. *Nature* **2001**, *414*, 353.
(2) Satyapal, S.; Petrovic, J.; Read, C.; Thomas, G.; Ordaz, G. *Catal. Today* **2007**, *120*, 246.
(3) Meng, S.; Kaxiras, E.; Zhang, Z. *Nano Lett.* **2007**, *7*, 663.
(4) Xiong, Z. T.; Yong, C. K.; Wu, G. T.; Chen, P.; Shaw, W.; Karkamkar, A.; Autrey, T.; Jones, M. O.; Johnson, S. R.; Edwards, P. P.; David, W. I. F. *Nat. Mater.* **2008**, *7*, 138.
(5) Banerjee, S.; Murad, S.; Puri, I. K. *Proc. IEEE* **2006**, *94*, 1806.
(6) Xiong, Z. T.; Wu, G. T.; Hu, J. J.; Liu, Y. F.; Chen, P.; Luo, W. F.; Wang, J. *Adv. Funct. Mater.* **2007**, *17*, 1137.
(7) Nikitin, A.; Li, X. L.; Zhang, Z. Y.; Ogasawara, H.; Dai, H. J.; Nilsson, A. *Nano Lett.* **2008**, *8*, 162.
(8) Durgun, E.; Ciraci, S.; Zhou, W.; Yildirim, T. *Phys. Rev. Lett.* **2006**, *97*, 226102.
(9) Dillon, A. C.; Jones, K. M.; Bekkedahl, T. A.; Kiang, C. H.; Bethune, D. S.; Heben, M. *Nature* **1997**, *386*, 377.
(10) van Setten, M. J.; de Wijs, G. A.; Brocks, G. *Phys. Rev. B* **2007**, *76*, 075125.
(11) Liu, C.; Fan, Y. Y.; Liu, M.; Cong, H. T.; Cheng, H. M.; Dresselhaus, M. S. *Science* **1999**, *286*, 1127.
(12) Cho, J. H.; Park, C. R. *Catal. Today* **2007**, *120*, 407.
(13) Durgun, E.; Ciraci, S.; Yildirim, T. *Phys. Rev. B* **2008**, *77*, 085405.
(14) Pupysheva, O. V.; Farajian, A. A.; Yakobson, B. I. *Nano Lett.* **2008**, *8*, 767.
(15) Kuc, A.; Zhechkov, L.; Patchkovskii, S.; Seifert, G.; Heine, T. *Nano Lett.* **2007**, *7*, 1.
(16) Chandrakumar, K. R. S.; Ghosh, S. K. *Nano Lett.* **2008**, *8*, 13.
(17) Yoon, M.; Yang, S.; Hicke, C.; Wang, E.; Geohegan, D.; Zhang, Z. *Phys. Rev. Lett.* **2008**, *100*, 206806.
(18) Cabria, I.; López, M. J.; Alonso, J. A. *J. Chem. Phys.* **2005**, *123*, 204721.
(19) Rojas, M. I.; Leiva, E. P. M. *Phys. Rev. B* **2007**, *76*, 155415.
(20) Park, N.; Hong, S.; Kim, G.; Jhi, S.-H. *J. Am. Chem. Soc.* **2007**, *129*, 8999.
(21) Coluci, V. R.; Braga, S. F.; Baughman, R. H.; Galvão, D. S. *Phys. Rev. B* **2007**, *75*, 125404.
(22) Mpourmpakis, G.; Tylianakis, E.; Froudakis, G. E. *Nano Lett.* **2007**, *7*, 1893.
(23) Zhou, B.; Guo, W.; Tang, C. *Nanotechnology* **2008**, *19*, 075707.
(24) Yildirim, T.; Ciraci, S. *Phys. Rev. Lett.* **2005**, *94*, 175501.
(25) Sun, Q.; Jena, P.; Wang, Q.; Marquez, M. *J. Am. Chem. Soc.* **2006**, *128*, 9741.
(26) Stampfer, J. F.; Holley, C. E.; Suttle, J. F. *J. Am. Chem. Soc.* **1960**, *82*, 3504.
(27) Jhi, S.-H. *Phys. Rev. B* **2006**, *74*, 155424.
(28) Chen, P.; Wu, X.; Lin, J.; Tan, K. L. *Science* **1999**, *285*, 91.
(29) Yang, R. T. *Carbon* **2000**, *38*, 623.
(30) Pinkerton, F. E.; Wicke, B. G.; Olk, C. H.; Tibbetts, G. G.; Meisner, G. P.; Meyer, M. S.; Herbst, J. F. *J. Phys. Chem. B* **2000**, *104*, 9460.
(31) Perdew, J. P.; Wang, Y. *Phys. Rev. B* **1992**, *45*, 13244.
(32) Maresca, O.; Pellenq, R. J. M.; Marinelli, F.; Conard, J. *J. Chem. Phys.* **2004**, *121*, 12548.
(33) Chen, L.; Zhang, Y.; Koratkar, N.; Jena, P.; Nayak, S. K. *Phys. Rev. B* **2008**, *77*, 033405.
(34) Valencia, F.; Romero, A. H.; Ancilotto, F.; Silvestrelli, P. L. *J. Phys. Chem. B* **2006**, *110*, 14832.
(35) Klontzas, E.; Mavrandonakis, A.; Tylianakis, E.; Froudakis, G. E. *Nano Lett.* **2008**, *8*, 1572.
(36) Gao, G.; Çağin, T.; Goddard III, W. A. *Phys. Rev. Lett.* **1998**, *80*, 5556.
(37) Froudakis, G. E. *Nano Lett.* **2001**, *1*, 531.
(38) Krasnov, P. O.; Ding, F.; Singh, A. K.; Yakobson, B. I. *J. Phys. Chem. C* **2007**, *111*, 17977.
(39) Delley, B. *J. Chem. Phys.* **1990**, *92*, 508.
(40) Delley, B. *J. Chem. Phys.* **2000**, *113*, 7756.
(41) Yoon, M.; Yang, S.; Wang, E.; Zhang, Z. *Nano Lett.* **2007**, *7*, 2578.
(42) Cobian, M.; Iniguez, J. *J. Phys.: Condens. Matter* **2008**, *20*, 285212.
(43) Henwood, D.; Carey, J. D. *Phys. Rev. B* **2007**, *75*, 245413.
(44) Ataca, C.; Aktürk, E.; Ciraci, S.; Ustunel, H. *Appl. Phys. Lett.* **2008**, *93*, 043123.
(45) de Andres, P. L.; Ramírez, R.; Vergés, J. A. *Phys. Rev. B* **2008**, *77*, 045403.
(46) Wu, X.; Yang, J. L.; Zeng, X. C. *J. Chem. Phys.* **2006**, *125*, 044704.
(47) Deng, W.-Q.; Xu, X.; Goddard, W. A. *Phys. Rev. Lett.* **2004**, *92*, 166103.
(48) Zhou, Z.; Zhao, J.; Gao, X.; Chen, Z.; Yan, J.; Schleyer, P. v. R.; Morinaga, M. *Chem. Mater.* **2005**, *17*, 992.
(49) Huber, K. P.; Herzberg, G. *Molecular Spectra and Molecular Structure. IV. Constants of Diatomic Molecules*; Van Nostrand: New York, 1979.
(50) Li, J.; Furuta, T.; Goto, H.; Ohashi, T.; Fujiwara, Y.; Yip, S. *J. Chem. Phys.* **2003**, *119*, 2376.
(51) Askeland, D. R.; Phulé, P. P. *The Science and Engineering of Materials*, 4th ed.;Thomson Brooks/Cole: Pacific Grove, CA, 2004.
(52) Wu, X.; Gao, Y.; Zeng, X. C. *J. Phys. Chem. C* **2008**, *112*, 8458.
(53) Dag, S.; Ozturk, Y.; Ciraci, S.; Yildirim, T. *Phys. Rev. B* **2005**, *72*, 155404.

JP8091418